[10] R. C. Stabler, Phys. Rev. 133, A1268 (1964).

[11] V. I. Ochkur and A. M. Petrun'kin, Opt. i Spektroskopiya 14, 457 (1963) [Opt. Spectry. (USSR) 14, 245 (1963)].

[12] L. Vriens, Phys. Rev. 141, 88 (1966).

[13] J. D. Garcia, E. Gerjuoy, and J. E. Welker, Phys. Rev. 165, 66 (1968).

[14] P. C. T. de Boer, Phys. Fluids 10, 2485 (1967).

[15] P. C. T. de Boer, Von Karman Institute for Fluid Dynamics, Technical Note No. 48, 1968 (unpublished).

[16] M. R. H. Rudge, Rev. Mod. Phys. 40, 564 (1968).

[17] M. J. Seaton, Planetary Space Sci. 12, 55 (1964).

[18] J. D. Garcia, E. Gerjuoy, and J. E. Welker, Phys. Rev. 165, 72 (1968).

[19] J. D. Garcia, Phys. Rev. 177, 223 (1969).

[20] M. Gryziński, Phys. Rev. 107, 1471 (1957).

[21] R. M. St. John, F. L. Miller, and C. C. Lin, Phys. Rev. 134, 888 (1969).

PHYSICAL REVIEW A VOLUME 1, NUMBER 6 JUNE 1970

Negative-Ion Reactions in NO-H_2O Mixtures[*]

L. J. Puckett and W. C. Lineberger[†]

U.S. Army Ballistic Research Laboratories, Aberdeen Proving Ground, Maryland 21005

(Received 12 December 1969)

A stationary afterglow system has been utilized to determine rate constants for thermal-energy negative-ion–molecule reactions in photoionized NO-H_2O mixtures. When the decay of the plasma is controlled by ambipolar diffusion of positive and negative ions, quantitative determination of rate constants is shown to be feasible. The plasma transition from electron–positive-ion ambipolar diffusive domination of the transport loss processes to domination by positive-ion–negative-ion ambipolar diffusion is explained by a model which includes the effects of negative-ion trapping. Prominant negative ions in the afterglow include NO_2^-, its hydrates, and clusters involving HNO_2. Reaction-rate constants for the processes $NO_2^- + H_2O + NO \rightarrow NO_2^- \cdot H_2O + NO$ and $Cl^- + H_2O + NO \rightarrow Cl^- \cdot H_2O + NO$ are found to be $1.3 \pm 0.3 \times 10^{-28}$ cm^6/sec and $3.4 \pm 1.3 \times 10^{-29}$ cm^6/sec at 293 K, respectively. Steady glows in NO-H_2O-O_2 mixtures revealed that NO_3^- and the impurity HCO_3^- also formed multiple hydrates and clustered with HNO_2. These results indicate that the terminal negative ions in the D-region of the ionosphere will likely be hydrated.

I. INTRODUCTION

Recently Lineberger and Puckett[1,2] reported stationary-afterglow measurements of NO^+ reactions leading to the formation of $NO^+ \cdot NO$, $NO^+ \cdot n(H_2O)$ and $H_3O^+ \cdot n(H_2O)$ ions in photoionized NO-H_2O mixtures. These investigations elucidated a mechanism by which NO^+ ions can be lost in reactions with atmospheric water vapor. As a consequence of these reactions it is understandable that NO^+ should not be regarded as a terminal positive ion in the *D* region of the ionosphere.

Ferguson[3] and LeLevier and Branscomb[4] have reviewed *D*-region negative-ion chemistry and concluded that the "terminal" negative ions are NO_2^- and NO_3^-. This conclusion was based on the observation that these ions are formed through chain-breaking reactions that do not permit the electron to be freed again. Therefore, in their context, "terminal" implies that the ions are indestructible except through ion-ion mutual-neutralization processes. We report results which demonstrate that both NO_2^- and NO_3^- ions do, however, undergo clustering reactions with H_2O and HNO_2 at 293 K.

The negative-ion–molecule reaction rate constants reported in this paper are the first such measurements known to the authors to be made using stationary-afterglow techniques. In order to obtain quantitative negative-ion reaction rate information from a stationary afterglow, it is necessary to make observations subsequent to the disappearance of electrons from the decaying plasma during the interval when positive-ion–negative-ion ambipolar diffusion is the dominant transport-loss mechanism. The transition from positive-ion–electron ambipolar diffusive domination to positive-ion–negative-ion ambipolar diffusive domination is marked by a sudden increase in the negative-ion wall current, and a sudden decrease in the positive-ion wall current. A model is presented which accounts for the features of this transition.

II. EXPERIMENTAL APPARATUS AND PROCEDURES

The basic apparatus employed in this experiment is the photoionized stationary-afterglow instrument described previously,[1] and only a brief account of the apparatus will be presented here. For the present work the mass filter was modified to permit observation of negative ions. A schematic diagram of the apparatus is shown in Fig. 1.

The afterglow cavity is an ultra-high-vacuum, bakeable, gold-coated stainless-steel cylinder 18 in. in diameter and 36 in. long. Information on the individual ion species in the plasma afterglow is obtained by means of time-resolved mass spectrometry of the ions which pass through a 0.60-mm-diam sampling orifice in the cavity wall. The sampling orifice is contained in a plate which is contoured to the shape of the cavity wall and electrically insulated from the wall. The potential on the plate is set at a variable but low attractive potential (<100 mV). The orifice plate potential did not affect the rate-constant determinations in this work; however, we have noted[1] that observed diffusion-loss rates are affected by the plate potential. Consequently, care must be exercised in all measurements of diffusion coefficients in cases where a draw-out potential is employed.

In this investigation the negative ions were formed by electron attachment in the gas. The electrons were produced by photoionization of NO by means of krypton resonance radiation (123.6 and 116.5 nm) from a pulsed microwave-powered discharge lamp. Initial ion density is sufficiently low ($\sim 10^6$ cm^{-3}) that recombination loss rates are negligible compared with reactive and diffusive loss rates.

The NO gas used in this work was processed in the following manner. Specially prepared gas of 99.9% stated purity was obtained from a steel cylinder. The gas was passed through a stainless-steel and glass line to a liquid-N_2 trap where it was condensed. By means of a stationary vapor bath[5] the trap temperature could be maintained within ±0.5 K of any desired temperature in the range 77 to ~300 K. The NO vapor at the selected trap temperature was passed through a servo-controlled leak valve to the afterglow chamber. The experimental results in this paper were found to be insensitive to trap temperatures below 200 K. Above this temperature trace amounts of NO_2 in the NO were not completely trapped and appeared as impurity ions in the afterglow. Water-vapor densities required for the rate-constant determinations were obtained in the manner described previously.[2]

III. AFTERGLOW ANALYSIS

Figure 2 shows the temporal profiles of the principal positive and negative ions in a photoionized NO afterglow at a total pressure of 50 mTorr. The primary ion NO^+ and its termolecular reaction to form $NO^+ \cdot NO$ have been discussed previously.[1] The principal negative ion observed was NO_2^-. The initial formation mechanism for NO_2^- is currently under investigation and will be reported in a future publication.

The temporal profiles in Fig. 2 show marked transitions in positive- and negative-ion behavior at ~170 msec. The transitions in the ion currents to the wall are associated with the transition in volume transport from electron-ion

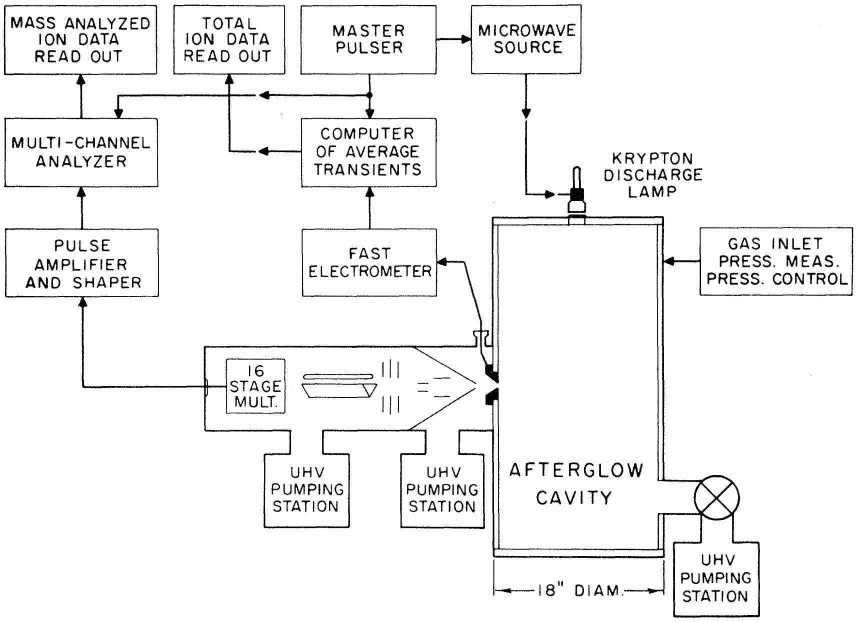

FIG. 1. Schematic diagram of stationary-afterglow apparatus.

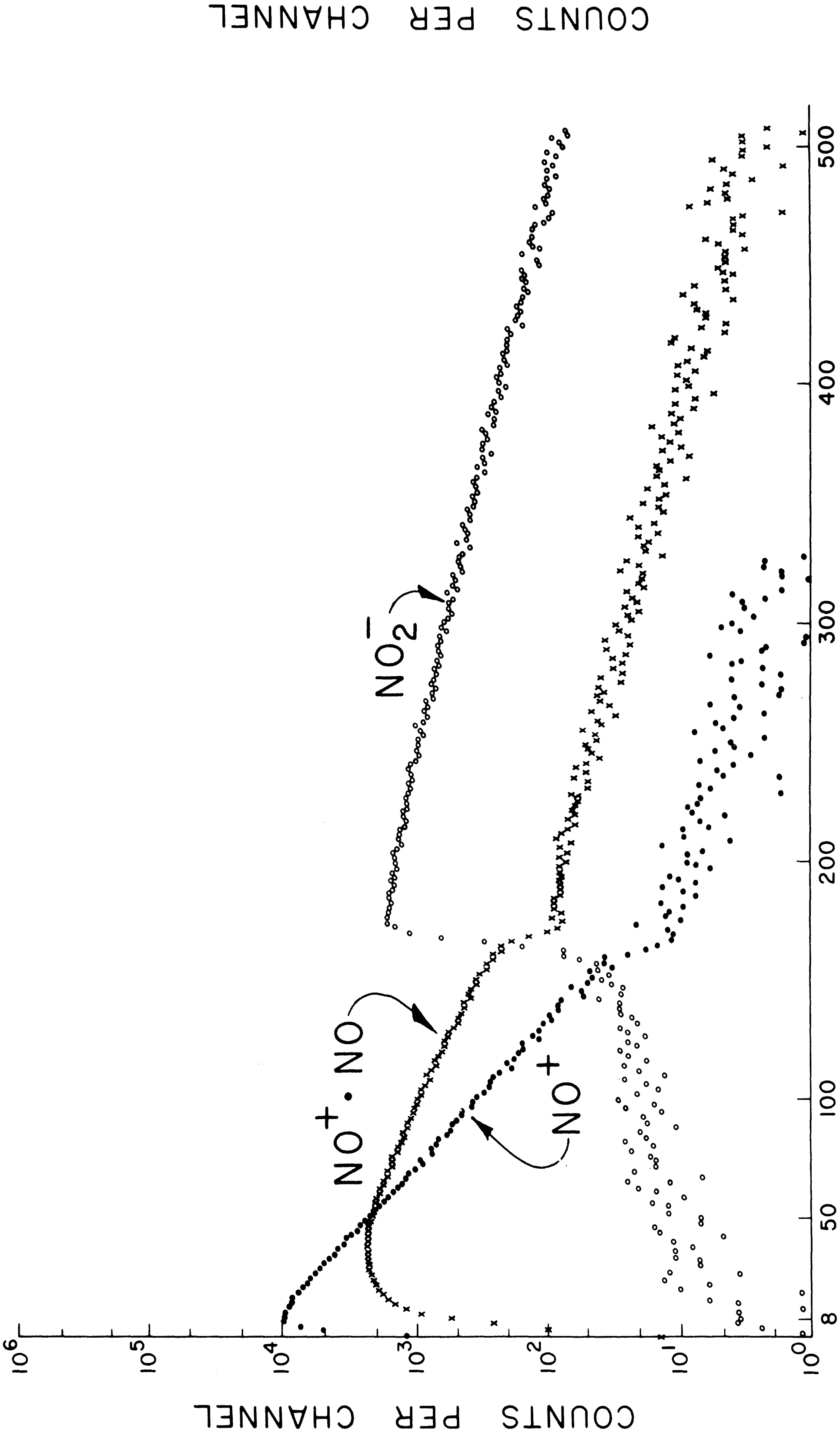

FIG. 2. Temporal afterglow profiles of NO^+, $NO^+ \cdot NO$, and NO_2^- wall currents at 50–mTorr NO pressure. (Pulse length is 8 msec; pulse interval is 1000 msec; orifice potential is ±50 mV.)

ambipolar diffusive domination to positive-ion–negative-ion ambipolar diffusive domination, and the resulting release of trapped negative ions. The trapping of negative ions prior to this transition, coupled with sampling discrimination effects, has thwarted previous efforts[6] to measure negative-ion–molecule reaction rates in stationary-afterglow experiments. In order to establish the validity of the reaction rate data presented here, it is necessary to investigate and explain the features of the transition. This section is accordingly devoted to an analysis of the plasma decay for times before, during, and after the transition.

In Fig. 2, for times <170 msec, the positive-ion decays are completely explained[1] by interconversion and positive-ion–electron ambipolar diffusive[7] loss. The principal features of the plasma decay that remain to be explained are as follows: (1) The negative-ion wall current increases sharply at 170 msec and then decays exponentially. (2) All ions decay exponentially with the same time constant after 170 msec. (3) Both of the positive-ion wall currents exhibit a sudden decrease by approximately a factor of 2 at 170 msec.

These features are all qualitative, explained in the context of a simple ambipolar diffusion model, as outlined below. The diffusion current density Γ of positive ions, negative ions, and electrons in the after glow may be expressed by[7]

$$\Gamma_+ = -D_+\nabla N_+ + N_+\mu_+ E\,, \tag{1}$$

$$\Gamma_- = -D_-\nabla N_- - N_-\mu_- E\,, \tag{2}$$

and $$\Gamma_e = -D_e\nabla N_e - N_e\mu_e E\,, \tag{3}$$

respectively. The quantities D and μ are free-diffusion coefficients and mobilities, while E is the electric field produced by noncharge neutrality in the plasma. The free-diffusion term $-D_i\,\nabla N_i$ is due to the density gradient of the ith charged species, while the mobility term $N_i\,\mu_i E$ describes the field-induced charged-particle drift in the gas. Although there are no applied electric fields in the afterglow, a "self-field" develops due to the initial rapid diffusion of electrons, producing a net charge separation which retards electron diffusion and enhances positive-ion diffusion. It may be shown[7] using the Einstein relation $\mu = eD/kT$ that the free-diffusion terms and the mobility terms are of equal magnitudes. For positive ions the mobility term produces a current in the same direction as that of free diffusion.

Hence, $$\Gamma_+ = -\,2D_+\,\nabla N_+ \equiv -D_{+\,,\,e}\,\nabla N_+\,, \tag{4}$$

where $D_{+\,,\,e}$ is defined as the positive-ion–electron ambipolar diffusion coefficient, and is equal to twice the free diffusion coefficient D_+.

In the case of electrons, the free-diffusion coefficient D_e and the mobility μ_e are a factor of 10^5 greater than those corresponding to ions in the afterglow. In spite of the fact that diffusion and mobility terms are in opposition for electrons, these terms are of sufficient magnitude that a departure of about 1 part in 10^5 from complete cancellation is adequate to maintain $\Gamma_e = \Gamma_+$.

In addition to being lost through positive-ion–electron diffusion, electrons are lost in attaching reactions which form negative ions. The electric field opposes the radial diffusion of negative ions, however, and as a result

$$\Gamma_- \simeq 0\,, \tag{5}$$

as can be seen in Fig. 2 for $t<170$ msec. In this sense the negative ions are trapped in the afterglow. Thus, the plasma decays through positive-ion–electron ambipolar diffusion until the number density of electrons is no longer sufficient to maintain the electric field which gave rise to ambipolar diffusion and negative-ion containment. The collapse of the electric field in the plasma is evidenced in the afterglow profile at $\simeq 170$ msec. According to Eq. (3), in the absence of the electric field, $\Gamma_e = -D_e\,\nabla N_e$ and the remaining electrons are lost very rapidly by free diffusive processes. In this simple model, the positive-ion diffusion current Γ_+ decreases from $2D_+\nabla N_+$ to $D_+\nabla N_+$, which gives rise to a rapid drop of wall current by a factor of 2 followed by a continued reduction by a factor of 2 in the exponential rate of plasma decay. Both of these features are apparent in the afterglow profile. The collapse of the E field also terminates the containment of the negative ions in the afterglow and produces a rapid increase of Γ_- from $\simeq 0$ to the value $\Gamma_- = -D\nabla N_-$, which in the first approximation is equal to Γ_+. These characteristics in the negative-ion behavior are also observable in the afterglow profile.

The relatively simple model described above qualitatively accounts for all of the observed transition features. A more refined numerical analysis of the transition has recently been completed by Kregel.[8] This refined calculation reproduces both the observed buildup of negative-ion current prior to the transition, and the smoothing of the transition observed in the positive-ion wall current.

IV. EXPERIMENTAL RESULTS AND DISCUSSION

These measurements are believed to constitute the first measurements of negative-ion reaction-rate constants to be obtained with a stationary-afterglow apparatus. Negative ions have been observed in other stationary-afterglow experiments,[6] but because of small signals and ion-discrimination effects, the previous observations were unable to follow the afterglow into the positive-ion–negative-ion ambipolar diffusion regime. Consequently for all times during the observations[6] there were both negative-ion sources, which were difficult to evaluate, and nonequilibrium ionic spatial distributions. As a result of these conditions meaningful negative-ion reaction-rate constants could not be obtained.

With the apparatus employed in this work the afterglow has been observed over seven decades of decay, four decades of which followed the electron-ion to ion-ion transition, i.e., four decades of decay in which there were negligible net sources of negative ions, and the ionic spatial distribution was a fundamental mode diffusive distribution.

Figure 3 shows the negative-ion spectrum in pure nitric oxide and in nitric oxide with varying amounts of water vapor. The dominant ion is NO_2^- followed in intensity by Cl^-. (The Cl probably originates in the AgCl cement used to attach the MgF_2 windows to the afterglow chamber.) In pure NO, NO_2^- is the dominant negative ion throughout the afterglow; however, when H_2O is added in small amounts other ions become prominant. Principal among these ions is $NO_2^- \cdot HNO_2$. Clusters of NO_2^- with H_2O become increasingly important as the water-vapor pressure increases. The hydrated NO_2^- and Cl^- are formed through the following reactions:

$$NO_2^- + H_2O + NO \xrightarrow{k_1} NO_2^- \cdot H_2O + NO, \tag{6}$$

$$Cl^- + H_2O + NO \xrightarrow{k_2} Cl^- \cdot H_2O + NO . \tag{7}$$

The rate constants k_1 and k_2 can be deduced through the following analysis.

If there are no NO_2^- sources and the dominant loss processes for NO_2^- ions in dilute H_2O-NO mixtures are positive-ion–negative-ion ambipolar diffusion and the reaction represented by Eq. (6), then for a fundamental mode diffusive distribution in a cylindrical cavity of radius R cm, the NO_2^- density in the afterglow may be expressed as

$$[NO_2^-(r,t)] = [NO_2^-(0,T)]J_0(2.405r/R) \times \exp\{-(D_{+,-}/\Lambda^2) - k_1[NO][H_2O]\}(t-T), \tag{8}$$

which is valid for $t > T$. Brackets [ ] denote the

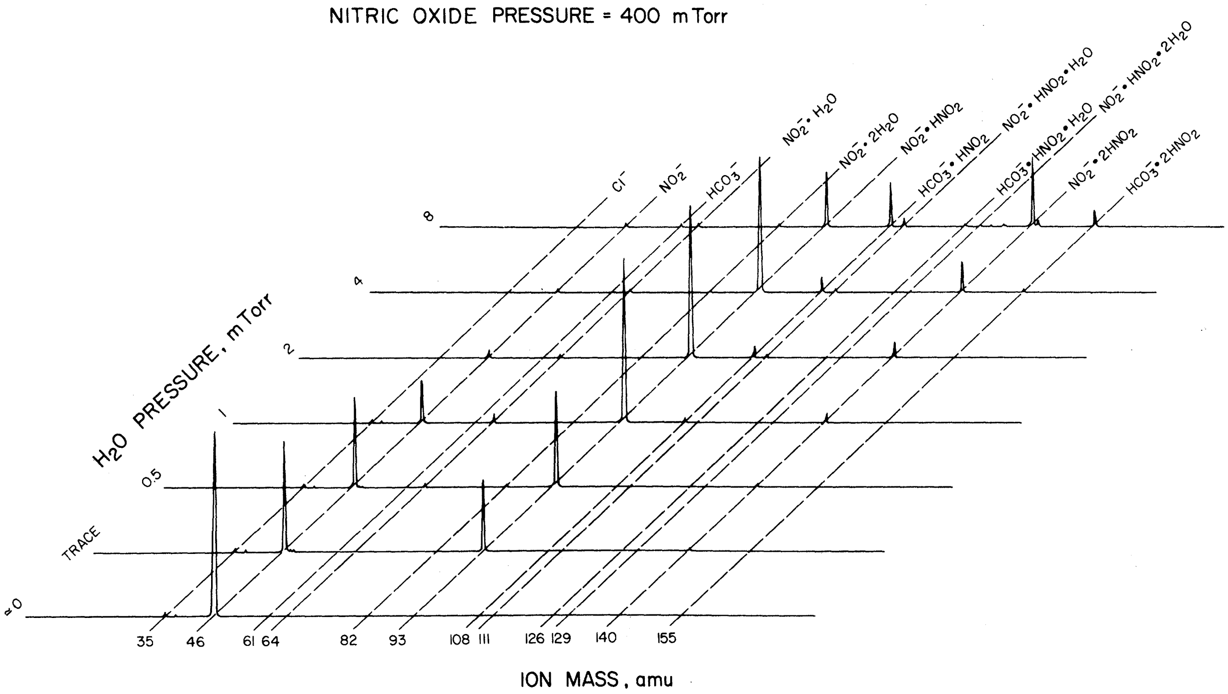

FIG. 3. Evolution of the negative-ion spectrum as a function of increasing H_2O concentration in NO at 400-mTorr NO pressure. The integrated spectrum for each H_2O concentration is normalized to the same value.

number density in cm^{-3}, $[NO_2^-(0, T)]$ is the axial number density at the time, T, of the transition from electron-ion to ion-ion ambipolar diffusion domination, and Λ is the characteristic diffusion length of the afterglow chamber.

It can be shown that under the proper experimental conditions,[1] the count rate of a mass-analyzed ionic species is directly proportional to the ionic volume number density of that species. If the reciprocal time constant for the observed decay of NO_2^- is denoted by ν, then

$$\nu = (D_{+,-}/\Lambda^2) + k_1[NO][H_2O]\,. \qquad (9)$$

When trace amounts of H_2O are added to the NO, $(D_{+,-}/\Lambda^2)$ is not significantly affected and the contribution of $k_1[NO][H_2O]$ to ν can be measured. A plot of $\nu - (D_{+,-}/\Lambda^2)$ as a function of $[NO][H_2O]$ will indicate the dependence of the reaction on the NO and H_2O concentrations, and from this information the rate constant k_1 can be evaluated. The experimental data shown in Fig. 4 yield a value of $k_1 = 1.30 \pm 0.3 \times 10^{-28}$ cm^6/sec. Employing the same analysis for the Cl^- reactions as that described for NO_2^- the rate constant for the hydration of Cl^- [Eq. (7)] was determined to be $k_2 = 3.4 \pm 1.3 \times 10^{-29}$ cm^6/sec. In order to deduce the sequence of reactions which produce the prominent ion $NO_2^- \cdot HNO_2$ the following observations were made:

(i) The NO_2^- count rate did not vary with either irradiation time (for times ≫ the characteristic lifetime of the ion in the system) or with the residence time of gas in the chamber.

(ii) The count rate of $NO_2^- \cdot HNO_2$, however, did increase as a function of irradiation time, but did not increase with residence time of the gas in the chamber.

Observations (i) and (ii), together, indicate that the reactant HNO_2 was produced through radiation chemistry. This conclusion is in accord with previous investigations[2] which delineated a source of HNO_2 through NO^+-H_2O gas-phase chemistry.

(iii) The exponential decay of $NO_2^- \cdot HNO_2$ in the afterglow is substantially slower than that of NO_2^-, and lends further support to the conclusion that $NO_2^- \cdot HNO$ is not produced in reactions of NO_2^- with the chamber walls, but rather in gas-phase reactions. Figure 4 of this paper reveals, however, that the dominant loss of NO_2^- in NO-H_2O mixtures is the reaction

$$NO_2^- + H_2O + NO \rightarrow NO_2^- \cdot H_2O + NO\,, \qquad (6)$$

and not directly through

$$NO_2^- + HNO_2 + NO \rightarrow NO_2^- \cdot HNO_2 + NO\,, \qquad (10)$$

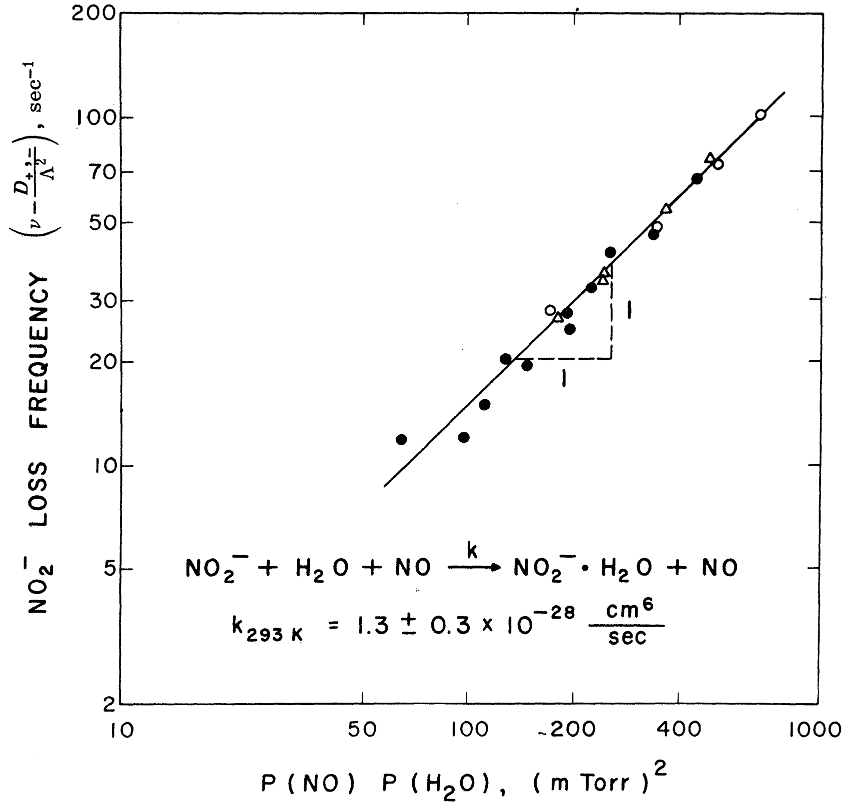

FIG. 4. Variation of NO_2^- reactive loss frequency as a function of the product of NO and H_2O pressures.

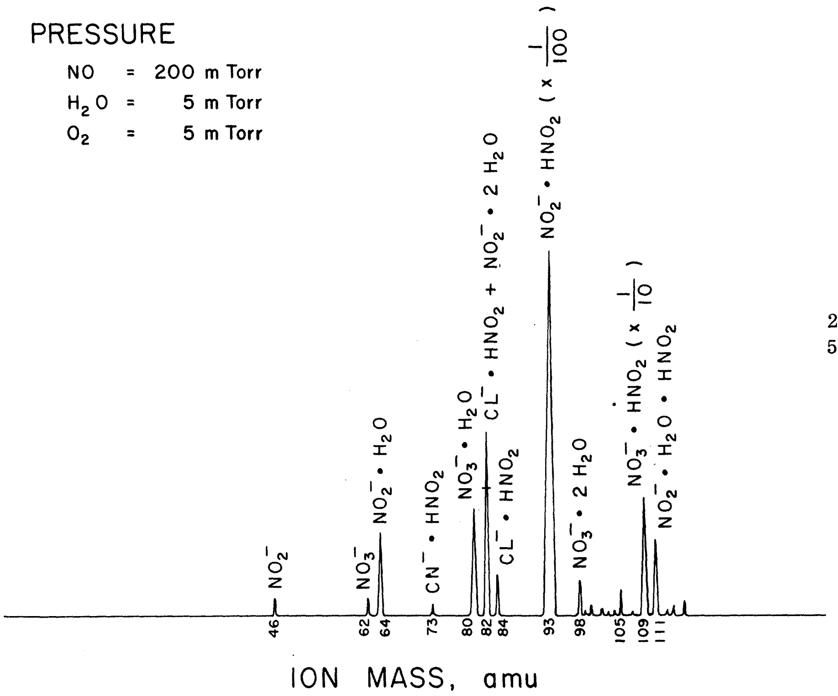

FIG. 5. Negative-ion spectrum in 200-m Torr NO, 5-m Torr H_2O and 5-m Torr O_2.

even though Fig. 3 indicates that the abundance of $NO_2^- \cdot HNO_2$ greatly exceeds that of $NO_2^- \cdot H_2O$. The indicated conclusion is therefore, that the principal source of $NO_2^- \cdot HNO_2$ is the reaction

$$NO_2^- \cdot H_2O + HNO_2 \rightarrow NO_2^- \cdot HNO_2 + H_2O\,, \qquad (11)$$

with reaction (10) being a minor source of $NO_2^- \cdot HNO_2$ under the conditions of this investigation. Reaction (11) is an example of the "switching" reactions recently reported by Adams *et al.*,[9] and the fact that reaction (11) is rapid indicates that the $NO_2^- \cdot HNO_2$ bond strength is greater than the $NO_2^- \cdot H_2O$ bond strength.

At the higher H_2O concentrations in Fig. 3 clustering reactions with both H_2O and HNO_2 prevail and the final negative ions are considerably more complex than NO_2^-. Similarly, clusters of the impurity HCO_3^- were observed to account for a large portion of the total ion spectrum at the higher water concentrations shown in Fig. 3. Further investigations revealed that NO_3^- present in NO-H_2O-O_2 mixtures (Fig. 5) also clustered with H_2O and HNO_2. In this figure tentative identifications are made based on mass-to-charge ratios.

The present findings serve to indicate that those ions previously designated as terminal negative ions in the *D* region of the ionosphere will certainly be hydrated, and perhaps clustering reactions with other *D*-region constituents will also be observed.

ACKNOWLEDGMENTS

The authors have profited from many stimulating discussions of the plasma transition with Dr. M. D. Kregel. M. W. Teague assisted in acquisition and interpretation of much of the experimental data. Appreciation is due Dr. F. E. Niles and Dr. G. E. Keller for numerous discussions concerning experimental results.

---

*Research supported in part by Defense Atomic Support Agency.

†Present Address: Joint Institute for Laboratory Astrophysics, University of Colorado, Boulder, Colo. 80302.

[1] W. C. Lineberger and L. J. Puckett, Phys. Rev. 186, 116 (1969).

[2] W. C. Lineberger and L. J. Puckett, Phys. Rev. 187, 286 (1969).

[3] E. E. Ferguson, Rev. Geophys. 5, 305 (1967).

[4] R. E. Lelevier and L. M. Branscomb, J. Geophys. Res. 73, 27 (1968).

[5] L. J. Puckett, M. W. Teague, and D. G. McCoy (unpublished).

[6] W. L. Fite and J. A. Rutherford, Discussions Faraday Soc. 37, 192 (1964).

[7] H. J. Oskam, Phillips Res. Rept. 13, 401 (1958).

[8] M. D. Kregel, J. Appl. Phys. (to be published).

[9] N. G. Adams, K. K. Bohme, D. B. Dunkin, F. C. Fehsenfeld, and E. E. Ferguson, J. Chem. Phys. (to be published).